Investigation of combustion of emulated biogas in a gas turbine test rig

Agustin Valera-Medina[1], Anthony Giles[1], Daniel Pugh[1], Steve Morris[1], Marcel Pohl[2], Andreas Ortwein[2,3]

[1] Cardiff University, Queen's Building, Cardiff CF24 3AA, United Kingdom
[2] DBFZ Deutsches Biomasseforschungszentrum gemeinnützige GmbH, Leipzig, Germany
[3] Hochschule Merseburg, Department Engineering and Natural Sciences, Merseburg, Germany

Abstract

Combustion of biogas in gas turbines is an interesting option for provision of renewable combined heat and power from biomass. Due to an increasing share of fluctuating renewable energies in the power grid (especially from wind and solar power), flexible power generation is of increasing importance. Additionally, with an increasing share of agricultural and municipal waste in biogas production, biogas composition is expected to be within a broader range.

In this paper, the combustion of synthetic biogas (carbon dioxide and methane) in a combustion test rig with a swirl burner and a high pressure optical chamber is researched at different conditions. Results are compared to a CHEMKIN-PRO simulation using a detailed reaction mechanism. The results show that within the researched experimental matrix, stable biogas combustion for gas turbines can be achieved even with significantly changing gas composition and nominal power. Carbon dioxide concentration is varied from 0 to 60 %. CO concentrations (normalized to 15 % O_2) in the flue gas do not change significantly with increasing carbon dioxide in the fuel gas and, for the researched conditions, staying below 10 ppm. NO_x concentration is below 10 ppm (normalized to 15 % O_2) for pure methane, and is furtherly decreasing with increasing carbon dioxide share in the fuel gas, which is mainly due to changing reaction paths as reaction analysis showed. Thermal load of the combustor is varied from 100 % to 20 % for the reference gas composition. With decreasing thermal load, normalized carbon monoxide flue gas concentration is furtherly reduced, while NO_x concentrations are remaining at a similar level around 5 ppm (normalized to 15 % O_2).

Keywords:
Gas turbine, biogas, combustion test, chemiluminescence

1. Introduction

Increasing the share of renewable energy is considered to be one of the main options to reduce greenhouse gas emissions, which are responsible for global warming. While solar and wind power are replacing more and more conventional power from fossil sources, they still show a volatile behaviour. Energy from biomass has the potential to provide power to the grid on demand [1-2] or via hybrid-technologies in combination with other renewable sources [3].

Electricity and, to a lesser extent, heat from anaerobic digestion have become a significant cornerstone in the energy systems, with (according to the European Biogas Association) roughly 10,000 biogas plants running in Europe alone. Biogas is produced by the biochemical conversion of biomass to methane and carbon dioxide under anaerobic conditions with the help of several microorganisms, especially bacteria and archaea. This fermentation process is usually divided into the four consecutive steps of hydrolysis, acidogenesis, acetogenesis/ dehydrogenation, and methanation [4]. Most of the installations for wet digestion are vertical continuous stirred tank reactors (CSTR) [5].

Biogas can be used directly or, after purification from carbon dioxide and trace gases (e.g. H_2S, NH_3), be injected into the natural gas grid as biomethane. Besides biogas upgrading for grid injection, there are several options for the conversion of biogas to electrical power [4]. Currently, the most common option is the use of gas engines [3, 6]. Other possibilities include fuel cells [7] and gas turbines, which can be used for a diversity of bio-fuels [8]. Biogas can also be used for direct provision of heat in gas boilers, although this application is rare due to the difference in achievable prices for electricity and heat [1].

Research on flexible biogas production has received increasing attention recently [1, 9-12].

Published version in: www.springer.com – Journal of Thermal Science
https://doi.org/10.1007/s11630-018-1024-1

Besides integration of further biogas storage capacities, implementation of power conversion units with comparably short reaction times are considered to be a main strategy for flexible power generation from biogas [11]. Technically, this development could benefit from the flexible operation of micro gas turbines. Although gas engines tend to have a slightly higher electrical efficiency compared to (micro) gas turbines [13], the latter promise to have significantly higher running times and availability, compared to gas engines.

Regarding large scale energy production systems, gas turbines for decentralized power production are available from below 30 kW_{el} [14] and are often referred to as micro gas turbines. High flexibility of these equipment has increased their usage with biogas and the research on this area.

In biogas production, concentrations of the main gases (methane and carbon dioxide) might change significantly with varying feedstock and process conditions, especially if considering the usage of agricultural residues and biogenic wastes in biogas production, but typically the methane content ranges between 45 and 65 % [15]. While for grid injection, the methane content only affects the technical upgrading efforts, it is expected to have significant effects in the direct usage in gas turbines. Another technical challenge in the application of micro gas turbines on anaerobic digestion plants is the higher sensitivity towards corrosive trace gases (e.g. siloxanes, [16]) in comparison to gas engines.

Somehsaraei *et al.* analysed the performance of a biogas-fuelled micro gas turbine (MGT) [17-18] focussing on the overall performance of the MGT and its modelling. They found the overall performance to be only slightly negatively influenced when using biogas instead of methane. Basrawi *et al.* [19] additionally included heating and cooling into the overall analysis and researched for the influence of ambient air temperature on electric and thermal efficiency. Their findings showed a decrease in electric efficiency and an increase in thermal efficiency with increasing ambient air temperature.

Lafay *et al.* [20] investigated the combustion of synthetic biogas and carbon dioxide diluted methane for gas turbines at atmospheric conditions. Their main findings were related to the study of the changes on equivalence ratio over flame stability. Mordaunt *et al.* [21] investigated different mixtures of CH_4 and CO_2 in a test rig under atmospheric conditions and with lower thermal input (up to 20 $L \cdot min^{-1}$ of CH_4 under standard conditions). Kang *et al.* [22] researched on the integration of biogas with different compositions into a MGT by simulating the gas turbine cycle. Iqbal *et al.* [23] also investigated different mixtures of CH_4 and CO_2, but concentrated on the comparison of numerical analysis with open source software OpenFOAM and experiments with an atmospheric combustor and different amounts of flue gas recirculation.

Further works have dealt with the measuring and modelling of burning velocities and NO formation in biogas combustion [24-25]. Also, the influence of hydrogen has been researched due to the strong influence of hydrogen on flame stability [26]. However, most literature has concentrated on the usage of these blends rather than on the characterisation of the burning process, essential component for power generation and emissions release. The aim of this study is to show the influence of different compositions of biogas on combustion in gas turbines at different loads. By changing carbon dioxide concentration in the fuel gas, results apply for exhaust gas recirculation (EGR), too. Combustion analysis is conducted by experimental methods in combination with kinetic simulation.

In section 2, a description of the test rig, the measurement methods, the experimental matrix and the simulation approach is given. The main results of the research are presented and discussed in section 3.

2. Method

2.1. Test rig description

The experiments for this study were conducted at Gas Turbine Research Centre at Port Talbot, Wales, UK, which is a research facility of Cardiff University [27-28]. The test rig used was the high pressure optical chamber (HPOC). It can be used with a maximum of 5 kg/s of air at 900 K and up to 16 bar(a). The generic pre-mixed swirl burner used for the experiments was designed to be working with gaseous fuels as well as with liquids (fig. 1). With the help of a quartz confinement tube, the expansion ratio between the burner outlet and the combustion chamber can be

Published version in: www.springer.com – Journal of Thermal Science
https://doi.org/10.1007/s11630-018-1024-1

simulated. The expansion ratio chosen for the experiments was 3.5, with a geometrical swirl number [29] of 1.04. The gases that were used were acquired from BOC Ltd (one of the main European gas suppliers) with a purity of 99.99 %.

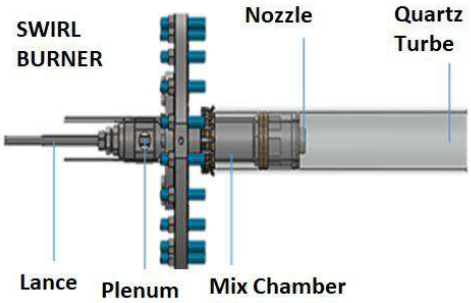

Fig. 1: *Generic swirl burner.*

2.2. Measurement methods

For the evaluation of liquid or gaseous fuel combustion in gas turbines, several measurement devices were applied to the HPOC. This includes basic optical equipment for flame recording, OH* (i.e. excited) chemiluminescence measurements, flue gas composition measurements, and temperature at the burner nozzle. Images of the flame were captured with video cameras from axial and radial positions. Flame colour, shape and stability were documented for evaluation. For all experiments, OH* chemiluminescence measurements were conducted to provide information about flame structure. To achieve this, a Dantec Dynamics Hi Sense Mk II CCD camera, having a resolution of 1.3 mega-pixel, was installed to take images through the top window of the test rig. This camera was coupled to a Hamamatsu C9546-03L image intensifier. A specialty 78 mm focal length lens (F-stop = f/3.8), that is capable of capturing light in the UV wavelength range, was installed on the image intensifier together with a narrow band pass filter centred at 307 nm with full width at half maximum (FWHM) of 10 nm. At each test point, 200 images were taken with a frequency of 10 Hz. Processing has been implemented by Dantec's DynamicStudio software with time-averaged images. All images were scaled to the same range.

Flue gas was analysed for NO_x, CO, CO_2 and O_2. The gas was sampled through a multi-point probe. The sample line and housing of that probe was held at 160 °C. NO_x was measured with a heated vacuum chemiluminescence analyser (Signal Instruments 4000VM NOx Analyzer) calibrated to 37.1 ppm NO and 1.9 ppm NO_2. The values were for dry gas and were normalized to 15 % oxygen. CO, CO_2 and O_2 were analysed by a Signal Instruments 9000M Multi Gas Analyzer, using an infrared cell for the first two and a paramagnetic sensor for oxygen. CO was calibrated for 0 – 900 ppm, CO_2 for 0 – 9 % and O_2 for up to 22.5 %. Again, values for CO and CO_2 were normalized to 15 % oxygen. Measurement error for the gas analysers was 5 %. Therefore, for the results, uncertainties of ±6% were produced as a consequence of errors in mass flow controllers (±0.5%), gas analysers and variance in atmospheric conditions during the tests.

Temperature was measured at several positions in the test rig. For this study, focus was on burner nozzle temperature which was measured with a type J thermocouple, since this temperature gave an indication about flash back of the flame.

2.3. Experimental matrix

For the design of the experimental matrix, several parameters were varied, which led to two sets of experiments. The experiments were conducted at atmospheric conditions. To account for changing biogas composition, concentrations of methane and carbon dioxide were changed (set 1). For reference composition, load was varied between 20 and 100 % (set 2). The full experimental matrix is listed in table 1, including adiabatic flame temperature T_{af} and associated thermal diffusivity α_{th}, thermal conductivity λ_{th}, kinematic viscosity ν and dynamic viscosity μ. The equivalence ratio φ, which is the ratio of stoichiometric combustion air to its actual amount, was set to φ =0.8 for this study. This value was chosen under consideration of the stability maps for emulated biogas under atmospheric conditions that can be found in literature [21].

2.4. Simulation approach

CHEMKIN-PRO was used to numerically determine the production of species and to understand major reaction patterns through the combustion of all different blends. For that aim, a hybrid Perfectly Stirred Reactor-Plug Flow Reactor (PSR-PFR) network was used and calibrated using pure methane under atmospheric conditions. High correlation (99 %) permitted evaluation of all mixed blends showing good agreement, as discussed in the following section. These networks have been commonly

Published version in: www.springer.com – Journal of Thermal Science
https://doi.org/10.1007/s11630-018-1024-1

used to simulate mixing and flow characteristics in gas turbine combustors [30].

Table 1. *Experimental matrix (Note: Test point 1-3 is identical with test point 2-1)*

Test point	CH4 [Vol%]	CO2 [Vol%]	P_{therm} [kW]	T_{af} [K]	α_{th} [m^2s^{-1}]	λ_{th} [$Wm^{-1}K^{-1}$]	ν [m^2s^{-1}]	μ [$kgm^{-1}s^{-1}$]
1-1	100	0	50	1996.6	0.000478	0.00671	0.000389	0.0000661
1-2	70	30	50	1929.4	0.000442	0.00650	0.000361	0.0000646
1-3	60	40	50	1894.2	0.000424	0.00638	0.000346	0.0000638
1-4	50	50	50	1847.2	0.000400	0.00623	0.000328	0.0000628
1-5	45	55	50	1817.3	0.000386	0.00614	0.000317	0.0000621
1-6	40	60	50	1781.6	0.000369	0.00602	0.000303	0.0000613
2-1	60	40	50	1894.2	0.000424	0.00638	0.000346	0.0000638
2-2	60	40	45	1894.2	0.000424	0.00638	0.000346	0.0000638
2-3	60	40	40	1894.2	0.000424	0.00638	0.000346	0.0000638
2-4	60	40	30	1894.2	0.000424	0.00638	0.000346	0.0000638
2-5	60	40	20	1894.2	0.000424	0.00638	0.000346	0.0000638
2-6	60	40	10	1894.2	0.000424	0.00638	0.000346	0.0000638

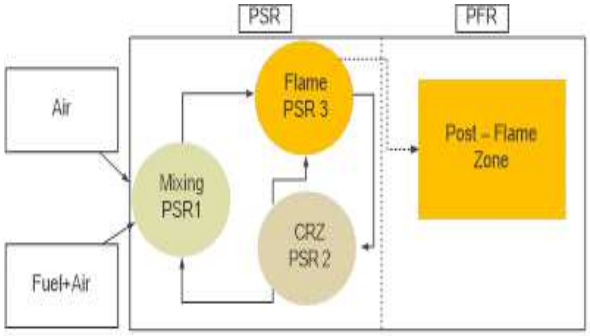

Fig. 2: *Gas turbine simulation network*

The network had two clusters, the first one representing the swirl burner with the existence of a central recirculation zone (CRZ) [30] with a recirculation set at 20 % of the product gases. Recirculation was approximated from previous experimental results obtained using the same device [31]. The second cluster was a Plug Flow Reactor that numerically accounts for the post-flame process along a 0.5 m duct, length of the experimental quartz tube used during the experimental campaign. Fig. 2 shows a schematic representation of the network. The numerical analysis was carried out with the GRI-MECH 3.0 chemical reaction mechanism, as this has been extensively used and proved for methane and hydrocarbon blends [32]. As part of the analysis, reaction pathways for main emission species are presented with a sensitivity analysis of the most important reactions when pure methane, a mixture of 40 % CH_4 and 60 % CO_2 and a mixture of 60 % CH_4 and 40 % CO_2 were used, thus allowing clear comparison between chemistry progression of these three cases. The results of the simulation have been normalized to 15 % of oxygen to compare them to experimental results.

3. Results and discussion

3.1. Emissions and flue gas composition

The results for NO_x emissions in relation to carbon dioxide content of the fuel gas can be seen in fig. 3. Contrary, carbon monoxide concentration (see fig. 4) is nearly constant for different carbon dioxide fuel gas concentrations. This phenomenon supports the previous statement, showing the same combustion efficiency for the reaction between O_2 and CH_4. Although CO_2 does not seem to be affecting the molecular interaction between species, i.e. producing the same CO concentration due to reaction between oxygen and methane, it does reduce the flame temperature, impacting only on NO_x and not CO.

The emissions at changing nominal power can be found in fig. 5 for carbon monoxide and in fig. 6 for NO_x. Due to increasing residence times coming with reduced flow, CO decreases as nominal power goes down.

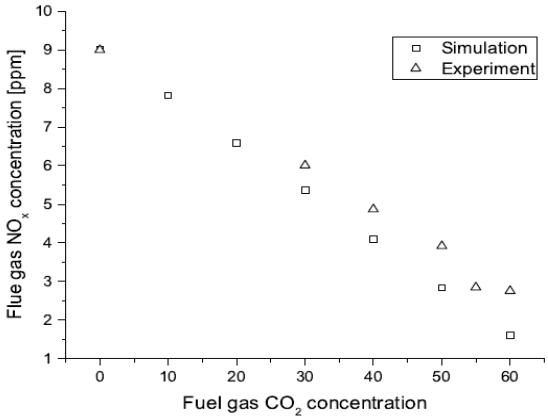

Fig. 3: *Experimental analysis and simulation of NO_x flue gas concentrations (normalized to 15 % O_2, dry) for different fuel gas compositions (test points 1-1 to 1-6)*

Published version in: www.springer.com – Journal of Thermal Science
https://doi.org/10.1007/s11630-018-1024-1

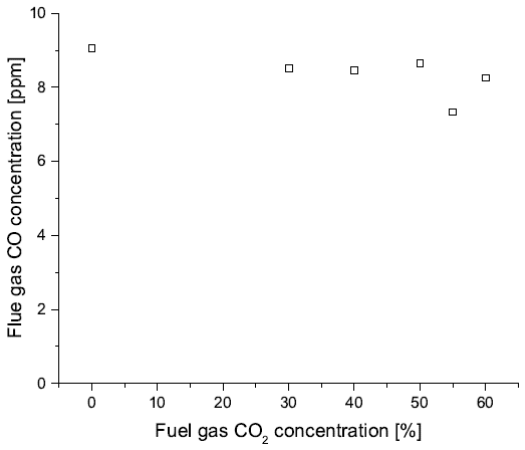

Fig. 4: *CO flue gas concentrations (normalized to 15 % O_2, dry) for different fuel gas compositions (test points 1-1 to 1-6)*

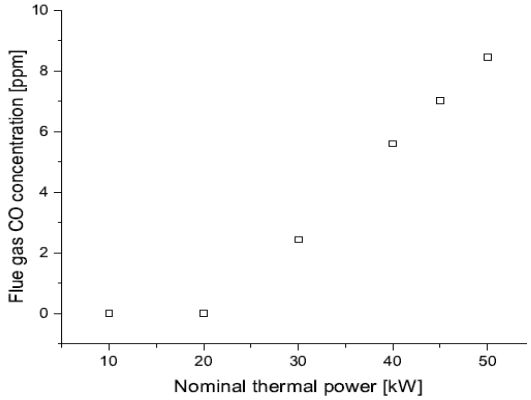

Fig. 5: *Carbon monoxide emission values (normalized to 15 % O2, dry) for different nominal power values at 40 Vol% of CO2 and 60 Vol.-% of CH4 (test points 2-1 to 2-6)*

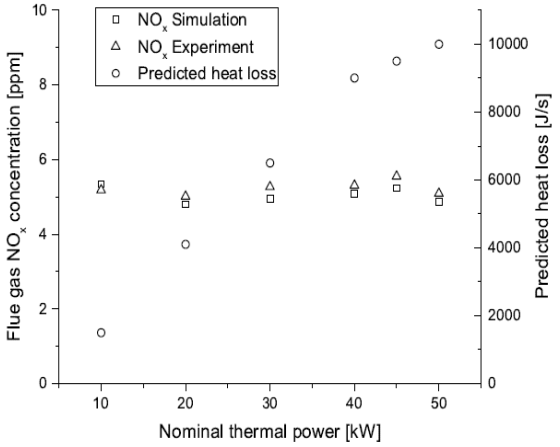

Fig. 6: *Experimental analysis and simulation of NOx flue gas concentrations (normalized to 15 % O2, dry) for different nominal power values at 40 Vol% of CO2 and 60 Vol% of CH4 (test points 2-1 to 2-6)*

However, NO_x remains at the same value even though power increases. For this condition, lower reaction (thus higher CO) keeps the flame at relatively lower temperatures even at higher power, effect that is enhanced by heat losses observed through the quartz at higher nominal powers, Fig. 6.

3.2. Chemiluminescence and optical observations

The chemiluminescence results (raw images and equivalent Abel deconvoluted images) for changing carbon dioxide rates in synthetic biogas are given in fig. 7.

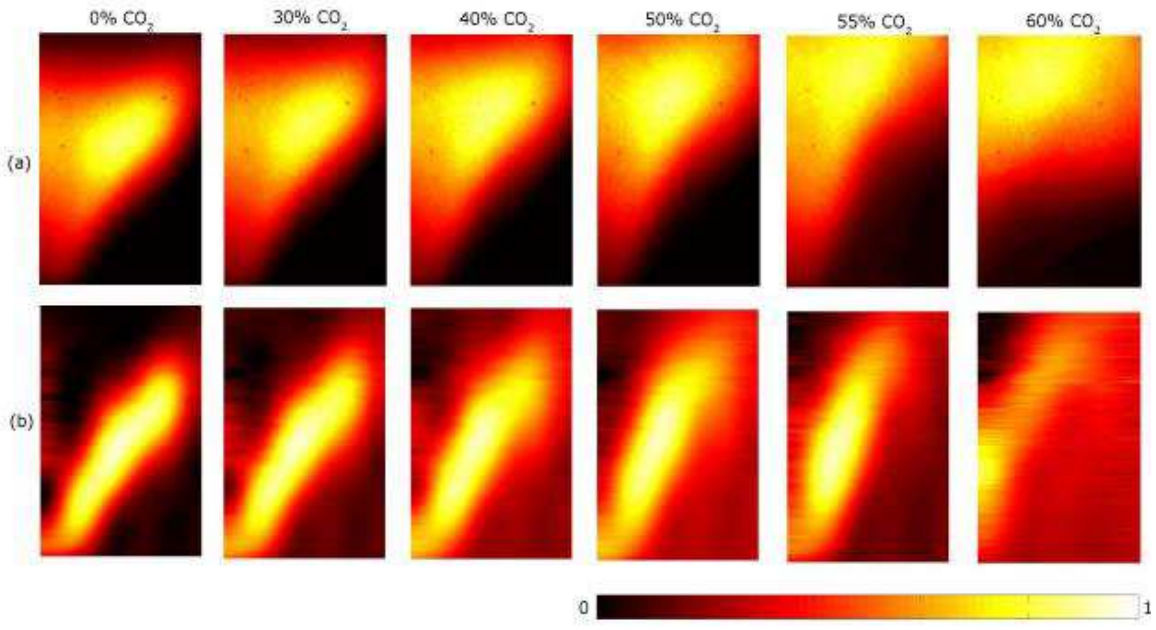

Fig. 7*: Average of 200 OH* chemiluminescence images (a), and equivalent Abel transformed images (b), depending on fuel gas CO2 content (test points 1-1 to 1-6)*

Published version in: www.springer.com – Journal of Thermal Science
https://doi.org/10.1007/s11630-018-1024-1

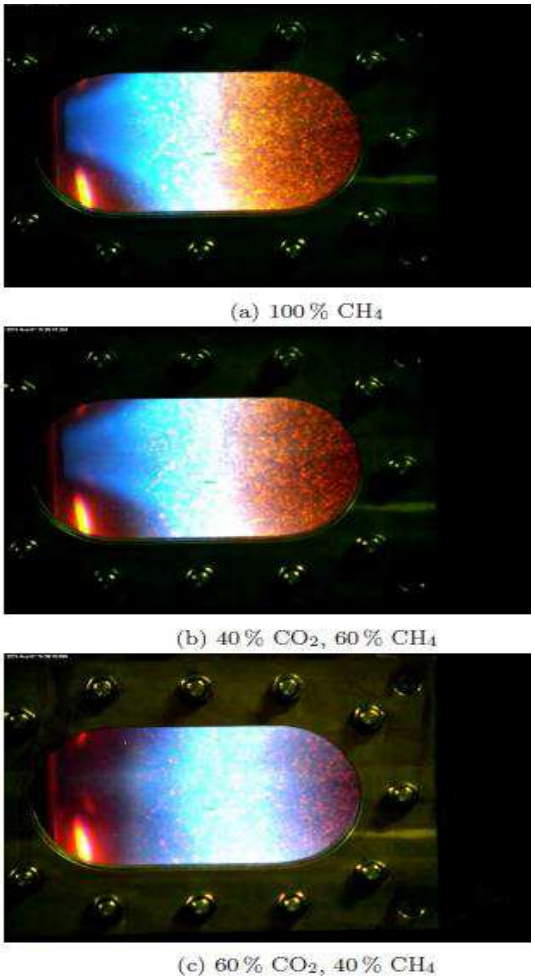

Fig. 8: *Axial flame observations for different fuel gas compositions (test points 1-1, 1-3 and 1-6).*

For all of the images, half of the flame is shown with image width of 49.5mm and image height of 75.4mm. All figures are oriented to present flow from bottom to top.

Under the given conditions, for a wide range (until 55% CO_2) a stable flame can be observed. With further increase in carbon dioxide concentration, the flame becomes unstable with a beginning blow-off. Typical examples for optical observations are given in fig. 8, where starting blow-off can be observed especially in fig. 8c.

The chemiluminescence results, again raw and equivalent Abel deconvoluted images, for changing nominal power in synthetic biogas are given in fig. 9. Image size and orientation are analogous to the results for changing fuel gas carbon dioxide content. Although the flame becomes weaker as expected, flame structure remains clearly recognisable with similar flame shape.

3.3. Burner nozzle temperature

Burner nozzle temperature showed nearly constant temperature for changing gas composition at 1 bar(a), until it reaches 60 % of CO_2, see fig. 10.

The sudden drop in temperature indicates that the flame is close to blow-off, which is in accordance to flame observations. With lowering

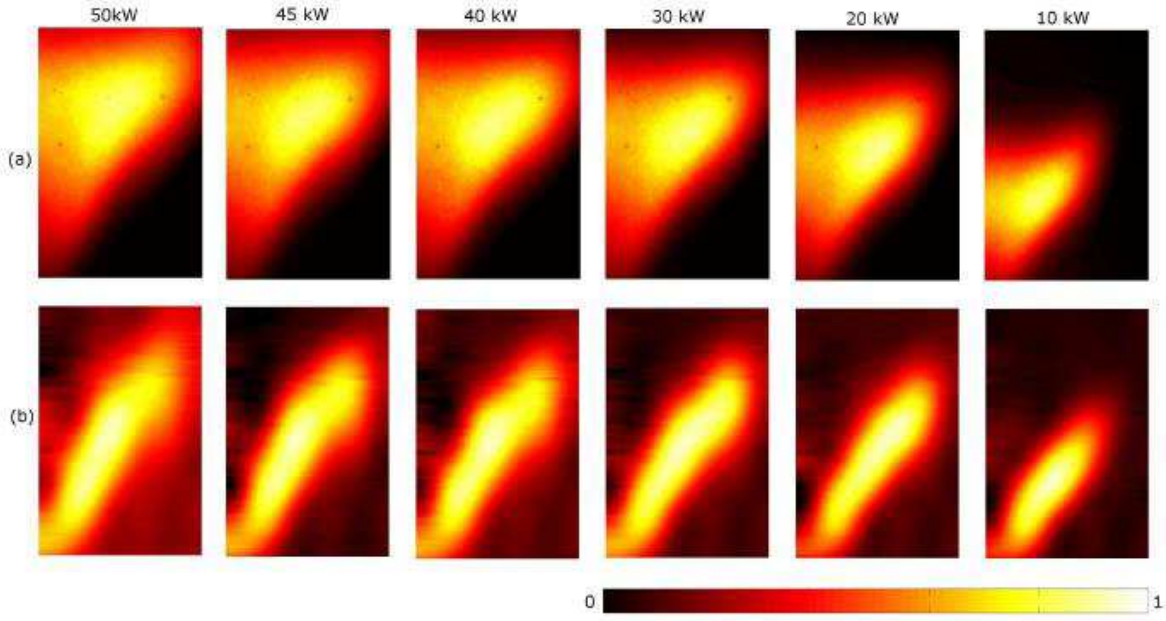

Fig. 9*: Average of 200 OH* chemiluminescence images (a), and equivalent Abel transformed images (b), depending on nominal thermal power (test points 2-1 to 2-6)*

Published version in: www.springer.com – Journal of Thermal Science
https://doi.org/10.1007/s11630-018-1024-1

nominal power (see fig. 11), burner nozzle temperature is decreasing, which is in accordance with heat loss prediction for these cases.

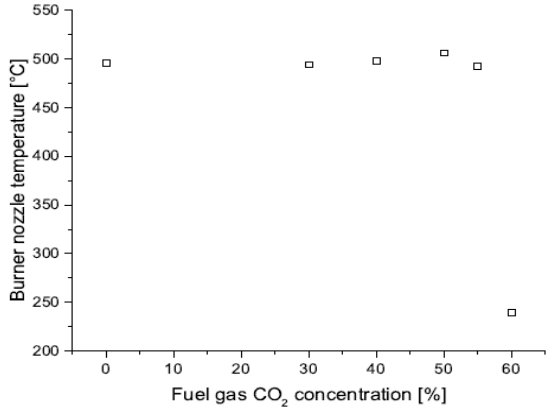

Fig. 10: *Burner nozzle temperature for different gas compositions (test points 1-1 to 1-6)*

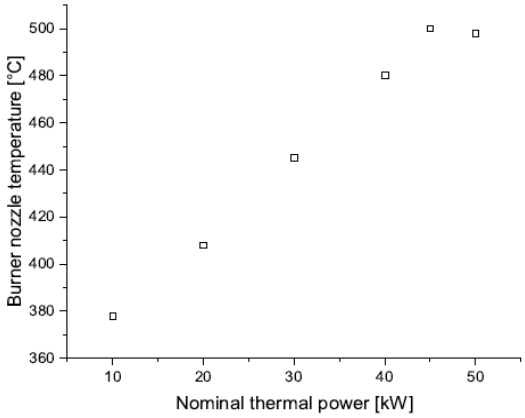

Fig. 11: *Burner nozzle temperature for changing nominal power (test points 2-1 to 2-6)*

3.4. Reaction analysis

Reaction analysis has been conducted for comparison of the combustion of 100 % CH_4, and mixtures of 60 % CH_4/40 % CO_2 and 40 % CH_4/60 % CO_2, respectively. Production rates for NO are given in fig. 12, while those for CO are given in fig. 13.

It was clear from the results that the mechanism of production of CO remained barely the same, with the reaction (1) being the most important for the production of species, and reaction (2) being the greatest consumer of carbon monoxide. Thus, it is clear that the addition of CO_2 into the blend has a minimal impact on the production of carbon monoxide at the same power conditions. This is a consequence of the production of OH and splitting of CH_3, which are independent of the carbon dioxide in the flow. At the same time, increased residence time leads to decreasing CO concentrations for lower thermal power.

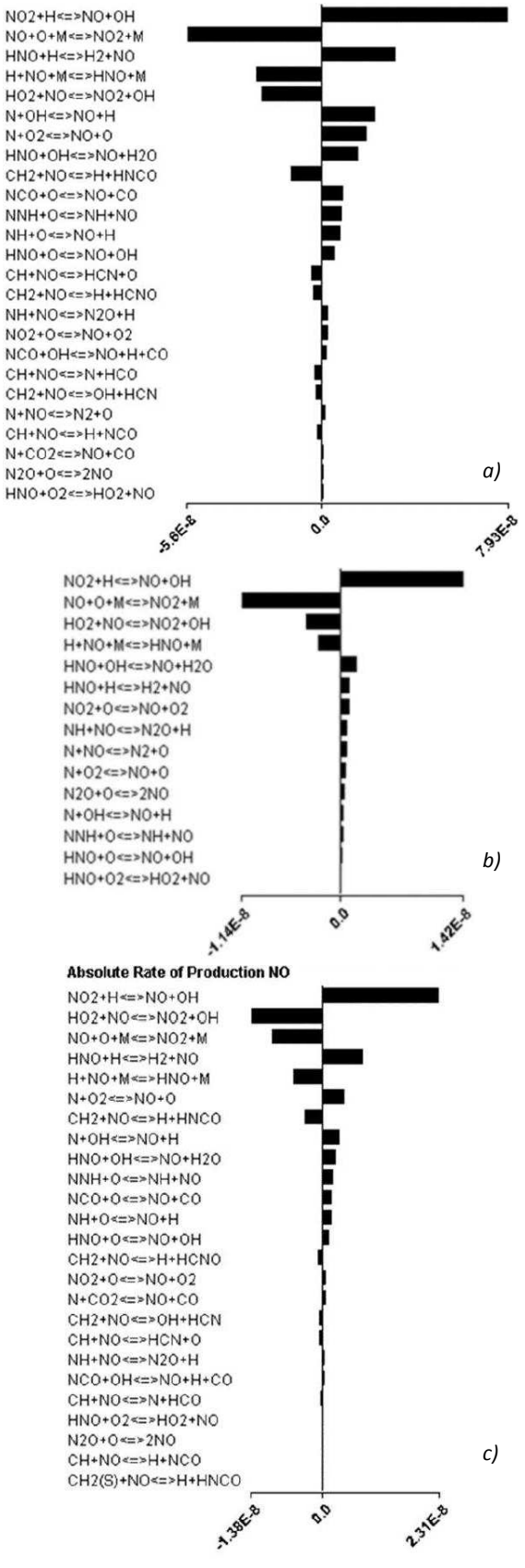

Published version in: www.springer.com – Journal of Thermal Science
https://doi.org/10.1007/s11630-018-1024-1

***Fig. 12**: Absolute production rates for NO for different gas compositions, a) 100% CH_4; b) 40% CO_2, 60% CH_4; c) 60% CO_2, 40%CH_4*

$$O + CH_3 \rightarrow H + H_2 + CO \quad (1)$$

$$OH + CO \rightarrow H + CO_2 \quad (2)$$

However, another scenario is perceived for NO. Contrary to CO, NO is highly susceptible to the presence of CO_2. Although the main reaction for the production of NO is always eq. (3), the consumption of the molecule shifts from eq. (4) to eq. (5) at high concentrations of CO_2 (60 %).

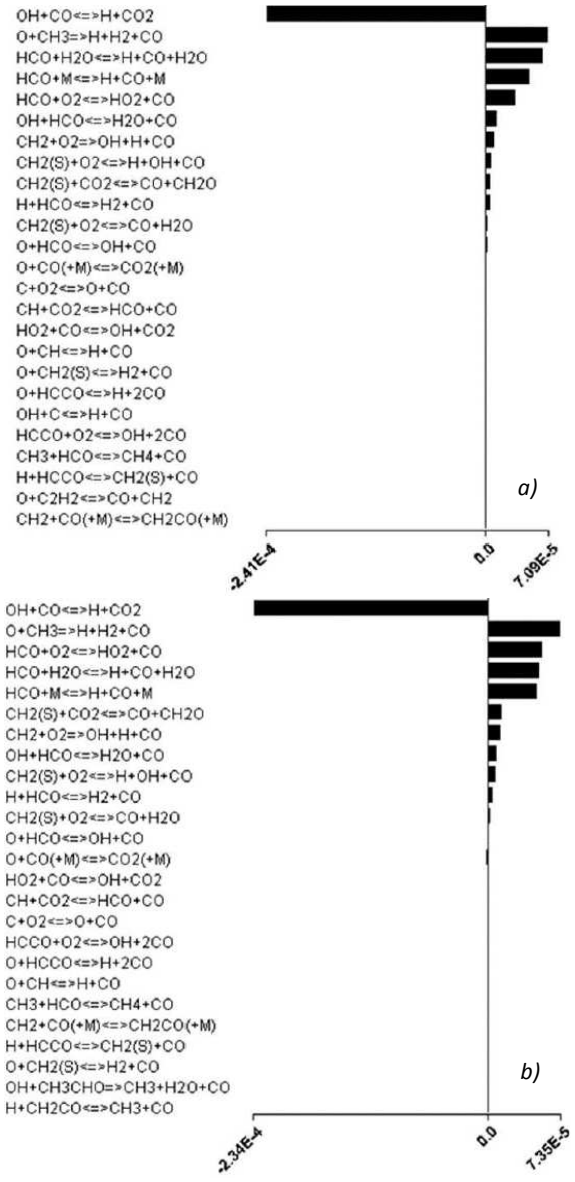

***Fig. 13:** Absolute production rates for CO for different gas compositions. a) 100% CH_4; b) 60% CO_2, 40%CH_4. Results for 40% CO_2, 60% CH_4 are almost identical to the latter.*

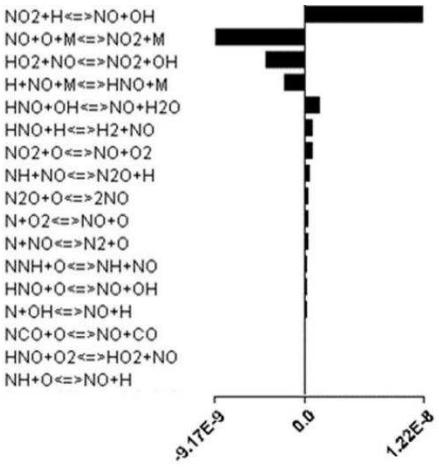

***Fig. 14:** Production rates for NO at nominal thermal power of 10 kW, with 60% CH_4 and 40% CO_2.*

As observed, the change in reaction is not monotonously. Although reaction (4) is still important for the consumption of the NO molecule, as the CO_2 concentration is increased the importance of the latest reaction is overthrown by reaction (5) as the main consumer of nitrogen oxides. For changing nominal power (see fig. 14) reaction paths for NO are nearly constant.

$$NO_2 + H \rightarrow NO + OH \quad (3)$$

$$NO + O + M \rightarrow NO_2 + M \quad (4)$$

$$HO_2 + NO \rightarrow NO_2 + OH \quad (5)$$

The reaction according to eq. (5) presents negative activation energies (i.e. -480 J/mol), different to eq. (4) with zero activation energy [32]. Therefore, as temperature in the system is increased, and more NO are present, eq. (4) leads the production of NO_2 with a decay response from eq. (5) due to higher temperatures. However, as temperature declines consequence of CO_2 increase, less NO will be present, eq. (5) will be enhanced, and with higher HO_2 radicals than O molecules in the blend post-combustion, eq. (5) will become the main consumer of NO. Other works [33] have also stated the relatively slower reaction of eq. (4) compared to other NO reactions during combustion, which could contribute to this behaviour. Although similar results have been documented somewhere else from experimental trials [34], these results demonstrate that the core reduction of NO relays on these reactions, being shifted on the basis of different working gases and temperatures. However, these effects require further

Published version in: www.springer.com – Journal of Thermal Science
https://doi.org/10.1007/s11630-018-1024-1

investigations to demonstrate this response to the changes in N_2/CO_2 concentration in the blend, as well as the playrole that N_2/CO_2 have in the third body *M* in such reaction.

3.5. Influence of composition and load change

With considerably increasing carbon dioxide content, the flame tended to lift-off at atmospheric conditions as well as at elevated pressure. The concentration at which lift-off could be noticed increased with pressure. Increasing carbon dioxide concentration showed a lowering in NO_x emissions, while CO emissions did not change significantly. Reaction pathways for NO_x are changing significantly with increasing CO_2, while those for CO are only slightly altered.

As previously mentioned, the initial flame sheet remains similar through all conditions, which is confirmed in fig. 10. Thus, CO_2 acts on the reduction of temperature downstream this point, barely affecting the combustion close to the nozzle.

According to these results, it can be assumed that combustion of biogas in gas turbine processes is relatively robust concerning changes in biogas composition within certain limits.

Changing the load of the combustion system is of interest due to an increasing share of volatile renewable energy sources in the grid, especially photovoltaics and wind. Reduction of load to 20 % of its nominal value was possible without problems. While NO_x emissions did not change much over the researched load range, CO emissions decreased towards zero. Burner nozzle temperature decreased gradually from 500 to 380 °C.

For the researched conditions, reducing load has no negative influence on emissions, promoting flexible operation of gas turbines. Nevertheless, reduction in temperature is expected to be negatively influencing electric efficiency, which is in accordance with existing research on biogas fuelled gas turbines [17] and should be considered in overall evaluation.

4. Conclusions

The combustion of simulated biogas under several conditions in a combustion test rig with a swirl burner and a high pressure optical chamber has been studied. The main focus was on changing fuel gas composition as well as fuel load. From the results, the following conclusions can be obtained:

- The results provisionally suggest that stable biogas combustion with low emissions may be achieved transitioning to gas turbine relevant conditions within a broad range of fuel gas carbon dioxide concentrations, thus providing robust operation of gas turbines with biogas from different sources and under different EGR conditions.
- Starting from below 10 ppm (normalized to 15 % O_2), NO_x concentrations decreased with fuel gas carbon dioxide concentration, while CO concentration did not change significantly and stayed below 10 ppm. Reaction analysis with simulation showed changing reaction paths for NO_x with increasing CO_2 concentration, while CO formation paths remained comparable.
- With reference composition (60 % CH_4, 40 % CO_2), load could be minimized to 20 % of nominal power with stable combustion. While electric efficiency is expected to decrease for these changes, emission values are not negatively influenced and, for carbon monoxide, even showed a further decrease.
- Heat loss prediction in reaction analysis for changing load is in accordance with temperature observations.

Acknowledgements

The authors gratefully acknowledge the support from the Biofuels Research Infrastructure for Sharing Knowledge (BRISK) 7th Framework Programme to conduct this project (ref. CFU3-01-09-15). The authors thank Terry Treherne and Jack Thomas for their invaluable contributions. The work was supported by funds of the Federal Ministry of Food and Agriculture (BMEL) based on a decision of the Parliament of the Federal Republic of Germany.

References

[1] Thrän, D. Smart Bioenergy *Springer International Publishing,* **2015**

[2] Thrän, D., Dotzauer, M., Lenz, V., Liebetrau, J., Ortwein, A. Flexible bioenergy supply for balancing fluctuating renewables in the heat and power sector - a review of technologies and concepts *Energy, Sustainability and Society,* **2015***, 5:35.*

[3] Gazda, W., Stanek, W. Energy and environmental assessment of integrated biogas trigeneration and

photovoltaic plant as more sustainable industrial system. *Applied Energy,* **2016***, 169*: 138 - 149

[4] Weiland, P. Biogas production: current state and perspectives. *Applied Microbiology and Biotechnology,* **2010***, 85*: 849 - 86

[5] Mao, C., Feng, Y., Wang, X., Ren, G. Review on research achievements of biogas from anaerobic digestion. *Renewable and Sustainable Energy Reviews,* **2015***, 45*: 540 - 555

[6] Lantz, M. The economic performance of combined heat and power from biogas produced from manure in Sweden – A comparison of different CHP technologies. *Applied Energy,* **2012***, 98*: 502 - 511

[7] Papurello, D., Borchiellini, R., Bareschino, P., Chiodo, V., Freni, S., Lanzini, A., Pepe, F., Ortigoza, G., Santarelli, M. Performance of a Solid Oxide Fuel Cell short-stack with biogas feeding. *Applied Energy ,* **2014***, 125*: 254 - 263

[8] Gupta, K. K., Rehman, A., Sarviya, R. M. Bio-fuels for the gas-turbine: A review. *Renewable and Sustainable Energy Reviews,* **2010***, 14*: 2946 - 2955

[9] Liebetrau, J., Daniel-Gromke, J., Jacobi, F. Flexible Power Generation from Biogas. In: Thrän, D. *(Ed.) Smart Bioenergy, Springer International Publishing,* **2015**: 67 – 82, Chapter 5

[10] Mauky, E., Jacobi, H. F., Liebetrau, J., Nelles, M. Flexible biogas production for demand-driven energy supply – Feeding strategies and types of substrates *Bioresource Technology,* **2015***, 178*: 262 - 269

[11] Hahn, H., Ganagin, W., Hartmann, K., Wachendorf, M. Cost analysis of concepts for a demand oriented biogas supply for flexible power generation. *Bioresource Technology,* **2014***, 170*: 211 - 220

[12] Hahn, H., Krautkremer, B., Hartmann, K., Wachendorf, M. Review of concepts for a demand-driven biogas supply for flexible power generation *Renewable and Sustainable Energy Reviews,* **2014***, 29*: 383 - 393

[13] Pöschl, M., Ward, S., Owende, P. Evaluation of energy efficiency of various biogas production and utilization pathways. *Applied Energy,* **2010***, 87*: 3305 - 3321

[14] Rasul, M., Ault, C., Sajjad, M. Bio-gas Mixed Fuel Micro Gas Turbine Co-Generation for Meeting Power Demand in Australian Remote Areas. *Energy Procedia,* **2015***, 75*: 1065 - 1071

[15] Dieckmann, C., Edelmann, W., Kaltschmitt, M., Liebetrau, J., Oldenburg, S., Ritzkowski, M., Scholwin, F., Sträuber, H., Weinrich, S. Biogaserzeugung und –nutzung In: Kaltschmitt, M.; Hartmann, H. & Hofbauer, H. *(Eds.)* Energie aus Biomasse *Springer Vieweg,* **2016**, 1609 - 1755

[16] de Arespacochaga, N., Valderrama, C., Raich-Montiu, J., Crest, M., Mehta, S., Cortina, J. Understanding the effects of the origin, occurrence, monitoring, control, fate and removal of siloxanes on the energetic valorization of sewage biogas—A review. *Renewable and Sustainable Energy Reviews,* **2015***, 52*: 366 - 381

[17] Somehsaraei, H. N., Majoumerd, M. M., Breuhaus, P., Assadi, M. Performance analysis of a biogas-fueled micro gas turbine using a validated thermodynamic model *Applied Thermal Engineering,* **2014***, 66*: 181 - 190

[18] Nikpey, H., Assadi, M., Breuhaus, P., Mørkved, P. Experimental evaluation and ANN modeling of a recuperative micro gas turbine burning mixtures of natural gas and biogas. *Applied Energy,* **2014***, 117*: 30 - 41

[19] Basrawi, F., Yamada, T., Nakanishi, K., Naing, S. Effect of ambient temperature on the performance of micro gas turbine with cogeneration system in cold region. *Applied Thermal Engineering,* **2011***, 31*: 1058 - 1067

[20] Lafay, Y., Taupin, B., Martins, G., Cabot, G., Renou, B., Boukhalfa, A. Experimental study of biogas combustion using a gas turbine configuration. *Experiments in Fluids,* **2007***, 43*: 395 - 410

[21] Mordaunt, C. J., Pierce, W. C. Design and preliminary results of an atmospheric-pressure model gas turbine combustor utilizing varying CO2 doping concentration in CH4 to emulate biogas combustion. *Fuel,* **2014***, 124*: 258 - 268

[22] Kang, D. W., Kim, T. S., Hur, K. B., Park, J. K. The effect of firing biogas on the performance and operating characteristics of simple and recuperative cycle gas turbine combined heat and power systems. *Applied Energy,* **2012***, 93*: 215 - 228

[23] Iqbal, S., Benim, A. C., Fischer Null, S., Joos, F., Kluß, D., Wiedermann, A. Experimental and Numerical Analysis of Natural Bio and Syngas Swirl Flames in a Model Gas Turbine Combustor. *Journal of Thermal Science,* **2016***, 25*:460 - 469

[24] Watson, G. M., Munzar, J. D., Bergthorson, J. M. NO formation in model syngas and biogas blends. *Fuel,* **2014***, 124*: 113 - 124

[25] Hinton, N., Stone, R. Laminar burning velocity measurements of methane and carbon dioxide mixtures (biogas) over wide ranging temperatures and pressures. *Fuel,* **2014***, 116*: 743 - 750

[26] Syred, N., Giles, A., Lewis, J., Abdulsada, M., Valera-Medina, A., Marsh, R., Bowen, P. J., Griffiths, A. J. Effect of inlet and outlet configurations on blow-off and flashback with premixed combustion for methane and a high hydrogen content fuel in a generic swirl burner. *Applied Energy,* **2014***, 116*: 288 - 296

[27] Valera-Medina, A., Morris, S., Runyon, J., Pugh, D. G., Marsh, R., Beasley, P., Hughes, T. Ammonia, Methane and Hydrogen for Gas Turbines *Energy Procedia,* **2015***, 75*: 118 - 123

[28] Valera-Medina, A., Marsh, R., Runyon, J., Pugh, D., Beasley, P., Hughes, T., Bowen, P. Ammonia-methane combustion in tangential swirl burners for gas turbine power generation. *Applied Energy,* **2017***, 185*: 1362 - 1371

Published version in: www.springer.com – Journal of Thermal Science
https://doi.org/10.1007/s11630-018-1024-1

[29] Claypole, T. C., Syred, N. The effect of swirl burner aerodynamics on NO_x formation *Symposium (International) on Combustion,* **1981***, 18*: 81 - 89

[30] Rutar, T., Malte, P. C. NOx Formation in High-Pressure Jet-Stirred Reactors With Significance to Lean-Premixed Combustion Turbines. *Journal of Engineering for Gas Turbines and Power,* **2002***, 124*: 776 - 783

[31] Syred, N. A review of oscillation mechanisms and the role of the precessing vortex core (PVC) in swirl combustion systems. *Progress in Energy and Combustion Science,* **2006***, 32*: 93 - 161

[32] Valera-Medina, A., Syred, N., Bowen, P. Central Recirculation Zone Visualization in Confined Swirl Combustors for Terrestrial Energy *Journal of Propulsion and Power,* **2013***, 29*: 195 - 204

[32] Smith, G. P., Golden, D. M., Frenklach, M., Moriarty, N. W., Eiteneer, B., Goldenberg, M., Bowman, C. T., Hanson, R. K., Song, S., Gardiner Jr., W. C., Lissianski, V. V., Qin, Z. GRI-Mech 3.0 http://www.me.berkeley.edu/gri_mech/ **1999**

[33] Ogryzlo, E.A., Schiff, H. I. The reaction of oxygen atoms with NO, Canadian Journal of Chemistry, **1959**, 37(10): 1690 – 1695

[34] Marsh R., Runyon J., Morris S., Pugh D., Valera-Medina A., Bowen P. Premixed methane oxycombustion in nitrogen and carbon dioxide atmospheres: measurements of operating limits, flame location and emissions. Proceedings of the Combustion Institute, 2017, 36(3): 3949 – 3958

Published version in: www.springer.com – Journal of Thermal Science
https://doi.org/10.1007/s11630-018-1024-1